

Deposition of Pt and Pt-Ru Nanoparticles on $\text{RuO}_2 \cdot x\text{H}_2\text{O}$ Using Microwave Method for Direct Methanol Fuel Cells

J. P. Zheng and V. Tiwari

Abstract—An easy and quick way to deposit platinum (Pt)-ruthenium (Ru) alloy nanoparticles on hydrous ruthenium dioxide ($\text{RuO}_2 \cdot x\text{H}_2\text{O}$) as supporting materials was developed using microwave heating. The x-ray diffractometer and selective area electron diffraction (SAED) showed that Pt-Ru alloy was formed. The transmission electron microscopic (TEM) image showed that average size of Pt-Ru was about 2-3 nm. Cyclic voltammogram of a Pt-Ru/ $\text{RuO}_2 \cdot x\text{H}_2\text{O}$ electrode showed high specific capacitance due to the protonation reaction in the acidic electrolyte and catalytic activity, including the methanol oxidation. The new Pt-Ru/ $\text{RuO}_2 \cdot x\text{H}_2\text{O}$ can be used as anode electrode materials in monolithic fuel cell/supercapacitor hybrid energy devices, since it has already been demonstrated that a layer of $\text{RuO}_2 \cdot x\text{H}_2\text{O}$ sandwiched between anode catalytic layer and a membrane improved the dynamic response of the direct methanol fuel cell (DMFC).

Index Terms—Direct methanol fuel cell, super capacitor, hybrid, and $\text{RuO}_2 \cdot x\text{H}_2\text{O}$.

I. INTRODUCTION

Among the different types of fuel cell, the direct methanol fuel cell (DMFC) has particular advantages including ease operation, miniaturization and a simple fuel supply system [1]-[4]. In recent years, research interest in high power DMFC modules has increased. This kind of power module is mainly designed for applications where high power mobile electrical energy sources are required (i.e. electrical vehicles and portable electronics devices) [1], [2], [5], [6]. Nevertheless, many problems relating to the operation of DMFCs under realistic operating conditions (i.e. dynamic operating conditions), have not been solved [7]-[11]. Therefore, all available fuel cell systems currently employ a large bank of battery or electrochemical (EC) capacitor between the electric load and fuel cell to buffer transient load demands [12], [13]. This buffer system brings the difficulties of further limiting the miniaturization of the fuel cell power system and lowering system cost. Therefore, it is attractive to be able to operate the DMFC system reliably and effectively without such a buffer system or at least with a much smaller one in order to widen the market for DMFC.

The poor performance of the DMFC is due to the poor kinetics of the anode reaction and fuel crossover [3], [14], [15]. Compared with losses in proton exchange membrane fuel cell (PEMFC) such as activation polarization, electrolyte ionic resistance, electrode ionic/ohmic resistance, DMFC also

includes larger anode activation overpotential and fuel crossover. The mass transport loss in DMFC is also much greater than that in PEMFC. The low catalyst utilization is due to the fact that only a relatively small amount of the catalyst surface materials are involved in direct contact with the three-phase boundaries consisting of proton conducting electrolyte, catalyst electrode, and fuel. More efficient use of the catalysts can be achieved by forming large surface area and electronic conductive carbon supported electrodes [16]. A primary role of the carbon support is to provide electrical connection between the widely dispersed catalyst particles and to be permeable to gases, water, and methanol. However, carbon itself does not conduct protons, which limits the achievable performance. Only those protons produced by the methanol electro-oxidation reaction near the membrane surface or within the diffusion length have a good chance to cross over the membrane to complete the reaction with oxygen in the cathode catalyst electrode. Such reactions are also limited to a thin layer near the membrane surface at the cathode side. Excessive Nafion was introduced into catalyst electrodes due to the electrode preparation in order to improve the proton conductivity in the catalyst electrodes; however, both the effective surface area of the catalyst nano-particles and the flow rate for fuel and gas are reduced due to decrease electrode porosity as a result of excessive Nafion, which covers the nano-particle surface.

It was proposed that the power performance of DMFC may be improved by introducing $\text{RuO}_2 \cdot x\text{H}_2\text{O}$ to totally or partially replace carbon support material in the anode electrode [17]. $\text{RuO}_2 \cdot x\text{H}_2\text{O}$ will not only play the role as a catalyst supporting material, but also as proton storage and a conductive medium. With a large number of protons stored in the anode electrode, the voltage and power stability of DMFC will be improved. The proton storage material of $\text{RuO}_2 \cdot x\text{H}_2\text{O}$ dynamically delivers protons and retards any decrease in voltage (power) across the fuel cell with increasing fuel cell current or decreasing fuel cell concentration. Additionally, $\text{RuO}_2 \cdot x\text{H}_2\text{O}$ also stores protons and retards any increase in voltage (power) across the fuel cell with decreasing fuel cell current or increasing fuel cell concentration. The capacitive characteristic of $\text{RuO}_2 \cdot x\text{H}_2\text{O}$ will also compensate for the inductive characteristic of DMFC due to mass transport. The voltage overshoot and undershoot will disappear after decreasing and increasing current steps, respectively [17]. To demonstrate the basic concept mentioned above, we have modified DMFC with a layer of $\text{RuO}_2 \cdot x\text{H}_2\text{O}$ layer sandwiched between the anode catalyst layer and membrane [18]. The previous experimental results have shown that by adding a layer of $\text{RuO}_2 \cdot x\text{H}_2\text{O}$ between anode catalyst layer and membrane in a DMFC, the transient response has

Manuscript received November 10, 2015; revised March 10, 2016. This work was supported in part by the U.S. Army CERDEC.

J. P. Zheng and V. Tiwari are with the Department of Electrical and Computer Engineering, Florida State University, Tallahassee, FL, USA (e-mail: zheng@eng.fsu.edu, tiwarvi@eng.fsu.edu).

significantly improved [18]. However, the steady state performance is reduced because of the added ionic resistance of the $\text{RuO}_2 \cdot x\text{H}_2\text{O}$ layer. Two important experimental results can be summarized as follows: (1) the transient voltage response of the regular DMFC was significantly improved which showed no overshoot or undershoot and the voltage swing reduced under the response of 0.3 Hz current square pulses; and (2) the proton conductivity of $\text{RuO}_2 \cdot x\text{H}_2\text{O}$ layer was measured to be 5.3×10^{-3} S/cm, which is close to the resistance obtained from the mixture of Pt/C and Nafion ionomer [17]. Due to the proton resistive layer, the ohmic resistance of the cell increased with increasing the loading (thickness) of $\text{RuO}_2 \cdot x\text{H}_2\text{O}$ layer; therefore the output power decreased. In this paper, we will demonstrate a method to coat Pt or PtRu nanoparticles on the surface of $\text{RuO}_2 \cdot x\text{H}_2\text{O}$, which is used to replace carbon support material. It is believed that the new catalytic materials used as an anode electrode in DMFC can improve the transient and dynamic response and also does not scarify the steady state performance.

II. SAMPLE PREPARATION

It was known that the specific capacitance for both $\text{RuO}_2 \cdot x\text{H}_2\text{O}$ and RuO_2 dropped sharply when they were annealed above a critical temperature at which the crystalline structure started to form. Typically, the critical temperature was about 120-150°C [17]-[20]. It is important to develop a method for deposition of the catalysts at temperatures below the critical temperature. However, the conventional method for making Pt or PtRu on carbon black applied high temperature (such as >700°C) in order to thermally decompose metal-chloride components. After such high temperature annealing process, the specific capacitance of $\text{RuO}_2 \cdot x\text{H}_2\text{O}$ would be significantly reduced. A new method must be developed for making Pt or PtRu on $\text{RuO}_2 \cdot x\text{H}_2\text{O}$ at low temperature such as <150°C.

It was reported that the microwave was applied to the boiling temperature at which the metal nanoparticles are formed [21], [22]. The advantage of this method is that the solution will rapidly heat up and cool down (less than 1 minute) to accelerate the reduction of the metal precursor ions and the nucleation of the metal particle in order to guarantee the particle size on the order of nm. In addition, the homogeneous microwave heating could reduce the temperature and concentration gradients in the reacting sample solution, resulting in a more uniform environment for the nucleation and growth of metal particles; however, the disadvantage of this method is that temperature is difficult to control. Usually, the microwave will heat the solution rapidly to the boiling point. The most commonly used solution for this microwave method is ethylene glycol. At the boiling temperature of about 197.3 °C, the ethylene glycol decomposed homogeneously to release the reducing agent for metal ion reduction [23]. However, it is well above the critical temperature for $\text{RuO}_2 \cdot x\text{H}_2\text{O}$ crystallization. It was found that the specific capacitance of $\text{RuO}_2 \cdot x\text{H}_2\text{O}$ after boiling it with ethylene glycol was less than 100 F/g vs. 700 F/g before the boiling. This problem could be solved if the boiling point of ethylene glycol could be lowered to the limit where it would

not hamper the specific capacitance of $\text{RuO}_2 \cdot x\text{H}_2\text{O}$. Since ethylene glycol is completely soluble in water, its boiling point could be lowered to the desired value (between 197.3 and 100 °C) by adding suitable amount of de ionized water as shown in Fig. 1.

During the Pt deposition on $\text{RuO}_2 \cdot x\text{H}_2\text{O}$, 250 mg $\text{RuO}_2 \cdot x\text{H}_2\text{O}$ (annealed at 116°C for 20 hours) was mixed with 50 mL ethylene glycol and equivalent weight of de-ionized water (52 mL). The mixture was then sonicated for 30 minutes. 4.37 g chloroplatinic acid was added to this solution and the mixture was sonicated again for 30 minutes. Diluted NaOH solution (0.5 M/L) was added to the solution to keep the PH above 10. The solution was placed inside a home microwave and was heated for 70 seconds at high power. The solution was allowed to cool and filtered and washed with de-ionized water five times. Finally it was washed with ethanol, filtered and air dried at 70°C for 12 hours. The dried powder was weighed and platinum loading in the mix was calculated. Difference in weight indicated that more than 95% of available platinum was deposited, hence giving 39% Pt loading vs. total weight of $\text{RuO}_2 \cdot x\text{H}_2\text{O}$ and Pt. Anode catalyst ink was prepared by mixing the catalytic powder with isopropanol alcohol, few drops of Nafion which was deposited on glassy carbon electrode.

Similarly Pt-Ru alloy was deposited on $\text{RuO}_2 \cdot x\text{H}_2\text{O}$. 250 mg $\text{RuO}_2 \cdot x\text{H}_2\text{O}$ was mixed with 50 mL ethylene glycol and 52 mL de-ionized water. The solution was sonicated for 30 minutes and 2.882 g of chloroplatinic acid and 117.46 mg of anhydrous ruthenium chloride was added to it. These quantities of precursors were chosen to get a molar ratio of Pt and Ru as 1:1 (approximate). The washing and drying processes were the same as mentioned above.

Cyclic voltammetry (CV) tests on these in-house made materials and commercial samples of Pt-Ru/C and Pt/C were performed, with 0.5 M/L H_2SO_4 solution as the electrolyte and their catalytic activities were observed. Nitrogen gas was bubbled for 30 minutes through electrolyte in order to get rid of dissolved oxygen. The testing sample was pasted on a glassy carbon as a working electrode, platinum mesh was used as a counter electrode, and the saturated calomel electrode (SCE) was used as reference electrode. To study the methanol (CH_3OH) oxidation activity, similar experiments were carried out but with 0.5 M/L H_2SO_4 and 1 M/L CH_3OH as electrolyte.

III. RESULTS AND DISCUSSION

In this work we are using a thermal decomposition technique by means of microwave heating to deposit Platinum and Platinum-Ruthenium alloy directly on unsupported hydrous ruthenium dioxide, without damaging the high capacitive properties of hydrous ruthenium dioxide. Literature [2] shows that specific capacitance of pure $\text{RuO}_2 \cdot x\text{H}_2\text{O}$ could be significantly increased by annealing it at a certain temperature. The annealing temperature, however, will depend upon the particular batch of $\text{RuO}_2 \cdot x\text{H}_2\text{O}$, depending upon its preparation techniques etc. For this batch of $\text{RuO}_2 \cdot x\text{H}_2\text{O}$, sample annealed at 116°C was found to show a very good specific capacitance. Improvement in specific capacitance after annealing could be seen in Fig. 1(a) and Fig.

1(b). Table I shows the specific capacitances of samples of un-annealed $\text{RuO}_2 \cdot x\text{H}_2\text{O}$, $\text{RuO}_2 \cdot x\text{H}_2\text{O}$ annealed at 116°C , Pt deposited on $\text{RuO}_2 \cdot x\text{H}_2\text{O}$ annealed at 116°C using microwave heating and Pt-Ru alloy deposited on $\text{RuO}_2 \cdot x\text{H}_2\text{O}$ annealed at 116°C using microwave heating.

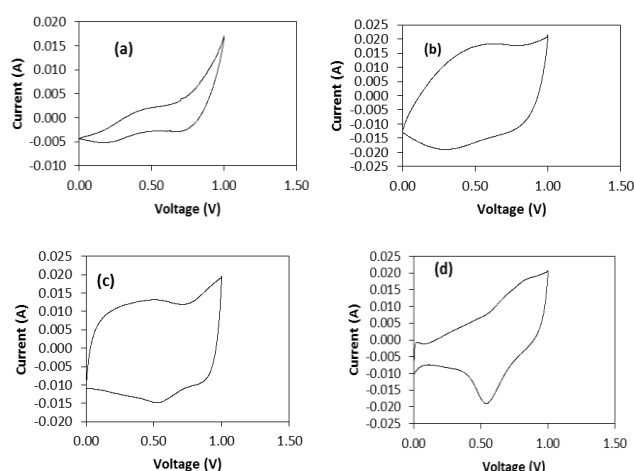


Fig. 1. Cyclic voltammograms, performed at the rate of 10mV/sec, to determine specific capacitance of (a) Pure $\text{RuO}_2 \cdot x\text{H}_2\text{O}$, (b) $\text{RuO}_2 \cdot x\text{H}_2\text{O}$ annealed at 116°C , (c) After depositing Pt (39%) on unsupported $\text{RuO}_2 \cdot x\text{H}_2\text{O}$ using microwave heating. (d) After depositing Pt-Ru alloy, Ru (13.65%) & Pt (26.35%), on unsupported $\text{RuO}_2 \cdot x\text{H}_2\text{O}$ using microwave heating.

TABLE I: SPECIFIC CAPACITANCES

Sample	Specific Capacitance measured
Un annealed $\text{RuO}_2 \cdot x\text{H}_2\text{O}$	161 F/g
$\text{RuO}_2 \cdot x\text{H}_2\text{O}$ annealed at 116°C	564 F/g
$\text{RuO}_2 \cdot x\text{H}_2\text{O}$, annealed at 116°C , after Pt has been deposited on it using microwave heating	604F/g
$\text{RuO}_2 \cdot x\text{H}_2\text{O}$, annealed at 116°C , after Pt-Ru has been deposited on it using microwave heating	700F/g

Ethylene glycol has been used as the reducing agent to reduce and thus deposit Pt from its precursor chloroplatinic acid and Ru from anhydrous ruthenium chloride on $\text{RuO}_2 \cdot x\text{H}_2\text{O}$. These reactions take place at high temperatures, and microwave heating is used to facilitate this. In order to achieve maximum loading, the mixture is to be heated to the point where ethylene glycol starts boiling. Therefore, the heating time in the microwave will depend upon the boiling point of ethylene glycol and total weight and volume of ingredients. As mentioned above, the annealing temperature used to obtain the high capacitance for this batch of $\text{RuO}_2 \cdot x\text{H}_2\text{O}$ was 116°C . Literature [2] shows that this temperature is fixed for particular batches of $\text{RuO}_2 \cdot x\text{H}_2\text{O}$ and heating it below or above that particular temperature may degrade its high capacitive properties. Therefore, the mixture of ethylene glycol, chloroplatinic acid and anhydrous Ruthenium Chloride, 0.5M NaOH (to maintain PH above 10) and $\text{RuO}_2 \cdot x\text{H}_2\text{O}$ is to be heated in the microwave to the point where it will surpass the boiling point of ethylene glycol i.e. 197.3°C . Heating at this temperature [2] may significantly affect (adversely) the capacitive properties of $\text{RuO}_2 \cdot x\text{H}_2\text{O}$. Also, the annealing temperature for $\text{RuO}_2 \cdot x\text{H}_2\text{O}$ varies from batch to batch². To overcome this problem, a method was

devised to control the boiling point of ethylene glycol using de-ionized water as a co-solvent. Different combinations of de-ionized water and ethylene glycol were taken and the variations in boiling point were noted, as shown in Fig. 2. Therefore, for this batch of $\text{RuO}_2 \cdot x\text{H}_2\text{O}$ (annealed at 116°C), ethylene glycol and de-ionized water were taken in ratio of 1:1 (by weight), which gives the boiling point of 108°C . This ratio seems perfect for this batch of $\text{RuO}_2 \cdot x\text{H}_2\text{O}$ because 108°C (boiling point of ethylene glycol mixed with de-ionized water in a ratio of 1:1) is lower than 116°C (annealing temperature to obtain high capacitive $\text{RuO}_2 \cdot x\text{H}_2\text{O}$), and therefore microwave heating (to be done to the point when the solution starts boiling, i.e. 108°C in this case) will not damage the high capacitive properties of $\text{RuO}_2 \cdot x\text{H}_2\text{O}$.

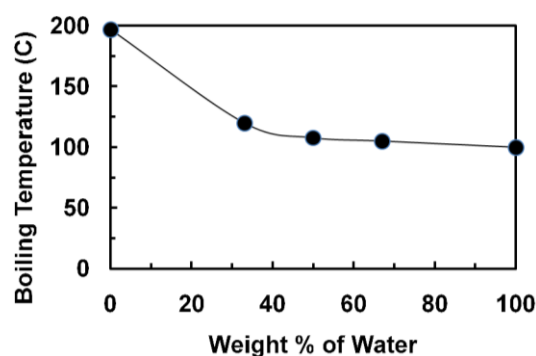


Fig. 2. The boiling points of different combinations of de-ionized water and ethylene glycol.

Please note that Table I shows specific capacitance of $\text{RuO}_2 \cdot x\text{H}_2\text{O}$ after Pt and Ru-Pt deposition using microwave heating method as slightly more than the plain sample of $\text{RuO}_2 \cdot x\text{H}_2\text{O}$ annealed at 116°C only. This increased capacitance could be owed to extra space charge added by the Platinum and or Ruthenium in the samples taken.

Cyclic voltammetry tests were performed on the samples prepared as discussed above and mentioned in experimental section i.e. Pt-Ru on $\text{RuO}_2 \cdot x\text{H}_2\text{O}$ and Pt on $\text{RuO}_2 \cdot x\text{H}_2\text{O}$. Fig. 3(a) and Fig. 3(b) shows that highly dispersed Pt and Pt-Ru has been deposited on $\text{RuO}_2 \cdot x\text{H}_2\text{O}$. For comparison purposes similar experiments were also performed on commercial ETEK samples of Pt-Ru (20% Pt, 10% Ru) on C as shown in Fig. 3(c) and Pt (20%) on C as shown in Fig. 3(d). Electrochemical surface areas using cyclic voltammetry (calculating the charge absorbed) were calculated [8] for all the four cases and are presented in Table II. Electrochemical surface areas calculated using this technique are showing lower values as per the standard values, most probably due to practical limitations in calculating the exact loading and the inability to obtain a uniform dispersed layer formation over the carbon glass electrode in the lab. But, under the same conditions, in-lab prepared Ru-Pt/ $\text{RuO}_2 \cdot x\text{H}_2\text{O}$ and Pt/ $\text{RuO}_2 \cdot x\text{H}_2\text{O}$ are giving comparable results to the commercial samples. Methanol oxidation activities, by calculating forward current peak to reverse current peak ratio were also calculated for all the samples, as shown in Fig. 4. It could be seen that Pt-Ru alloy (molar ratio 1:1 approx) deposited on $\text{RuO}_2 \cdot x\text{H}_2\text{O}$ gives much better methanol oxidation performance when compared to Pt directly deposited on $\text{RuO}_2 \cdot x\text{H}_2\text{O}$. This is of critical importance for materials to be used as catalysts in Direct Methanol fuel cells.

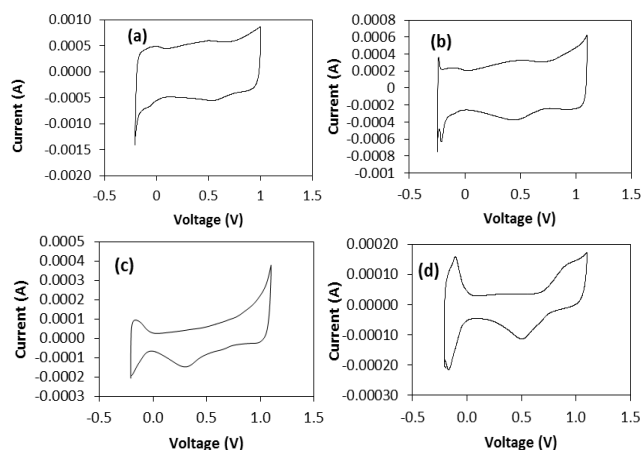


Fig. 3. Cyclic voltammograms, performed at the rate of 10mv/sec, to examine catalytic activity of (a) Pt deposited on $\text{RuO}_2 \cdot x\text{H}_2\text{O}$ ($[\text{Pt}] = 0.5772 \text{ mg/cm}^2$) using microwave thermal decomposition method, (b) Pt-Ru deposited on $\text{RuO}_2 \cdot x\text{H}_2\text{O}$ ($[\text{Pt}] = 0.2736 \text{ mg/cm}^2$) using microwave thermal decomposition method, (c) ETEK Pt-Ru (20%Pt, 10%Ru) /C ($[\text{Pt}] = 0.2 \text{ mg/cm}^2$), (d) ETEK Pt (20%)/C ($[\text{Pt}] = 0.2 \text{ mg/cm}^2$).

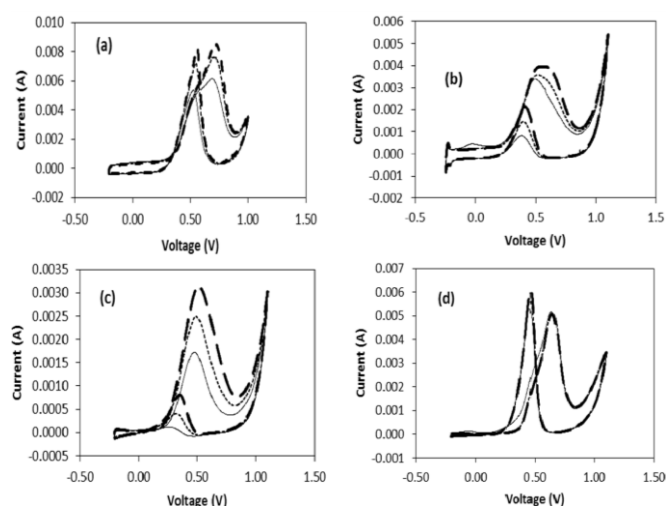


Fig. 4. Cyclic Voltammograms, performed at the rate of 10mv/sec, to examine methanol oxidation of (a) Pt(40%) deposited on $\text{RuO}_2 \cdot x\text{H}_2\text{O}$ ($[\text{Pt}] = 0.5772 \text{ mg/cm}^2$) using microwave thermal decomposition method, (b) Pt-Ru (26.35%Pt, 13.65%Ru) deposited on $\text{RuO}_2 \cdot x\text{H}_2\text{O}$ ($[\text{Pt}] = 0.2736 \text{ mg/cm}^2$) using microwave thermal decomposition method, (c) ETEK Pt-Ru (20%Pt, 10%Ru) /C ($[\text{Pt}] = 0.2 \text{ mg/cm}^2$), (d) ETEK Pt (20%)/C ($[\text{Pt}] = 0.2 \text{ mg/cm}^2$).

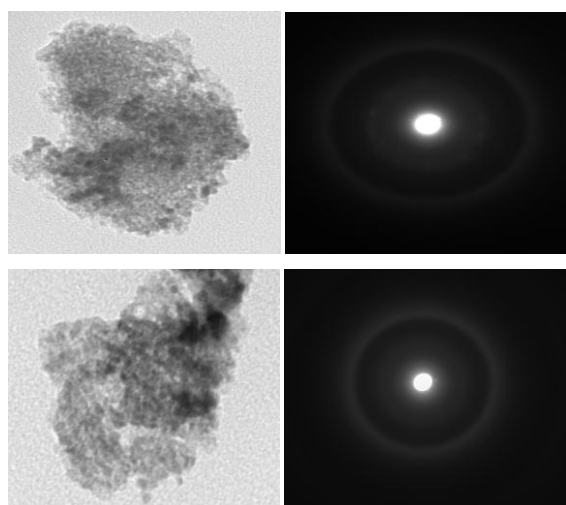


Fig. 5. (a) TEM image ($500,000\times$) of Pt/ $\text{RuO}_2 \cdot x\text{H}_2\text{O}$ (b) Electron diffraction ($500,000\times$) of amorphous looking region in the sample Pt/ $\text{RuO}_2 \cdot x\text{H}_2\text{O}$, confirming the presence of amorphous state of $\text{RuO}_2 \cdot x\text{H}_2\text{O}$ (c) TEM image($500,000\times$) of Pt-Ru/ $\text{RuO}_2 \cdot x\text{H}_2\text{O}$ (d) Electron diffraction ($500,000\times$) of amorphous looking region in the sample Pt-Ru/ $\text{RuO}_2 \cdot x\text{H}_2\text{O}$, confirming the presence of amorphous state of $\text{RuO}_2 \cdot x\text{H}_2\text{O}$.

TEM images, as shown in Fig. 5, of these in-lab prepared samples were taken and studied. It is seen that Ru in amorphous phase is present in both of the samples. Also, very small sized platinum particles (2 nm approx) are seen in these images, which is in agreement to the data obtained from XRD analysis.

TABLE II: ELECTROCHEMICAL SURFACE AREA AND METHANOL OXIDATION EVALUATION CALCULATING CHARGE ADSORBED DURING CYCLIC VOLTAMMETRY

Sample	ESA (m^2/g)	Forward current peak to backward current peak ratio
Pt (39%)/ $\text{RuO}_2 \cdot x\text{H}_2\text{O}$ using microwave thermal decomposition method	64.3	1.03
Pt (26.35%)-Ru (13.65%)/ $\text{RuO}_2 \cdot x\text{H}_2\text{O}$ using microwave thermal decomposition method	65.15	1.85
ETEK Pt-Ru (20%Pt, 10%Ru) /C	48.92	3.9
ETEK Pt (20%)/C	64.38	0.84

XRD Analysis — From the XRD performed on the sample of Pt deposited over $\text{RuO}_2 \cdot x\text{H}_2\text{O}$ using microwave heating, no peaks for anhydrous $\text{RuO}_2 \cdot x\text{H}_2\text{O}$ were obtained. A strong peak at $2\theta = 39.760$ confirms the presence of Pt, as shown in Fig. 6. The average particle size and surface area can be calculated from the equation:

$$d = \frac{k\lambda}{\beta \frac{1}{2} \cos \theta} \quad (1)$$

$$S = \frac{6000}{\rho d} \quad (2)$$

where d is the average particle size, λ is the wavelength of x-ray light (1.54 \AA), θ is the angle at the maximum peak, ρ is the density of Pt (21.4 g cm^{-3}) and $\beta \frac{1}{2}$ is the full width of the

half maximum (FWHM) of the diffraction peak. The average crystalline size calculated from Eqn. (1) is 2.82 nm and surface area as $99.42 \text{ m}^2 \text{ g}^{-1}$. This is an impressive value and shows the presence of highly dispersed Pt over $\text{RuO}_2 \cdot x\text{H}_2\text{O}$ in the sample prepared.

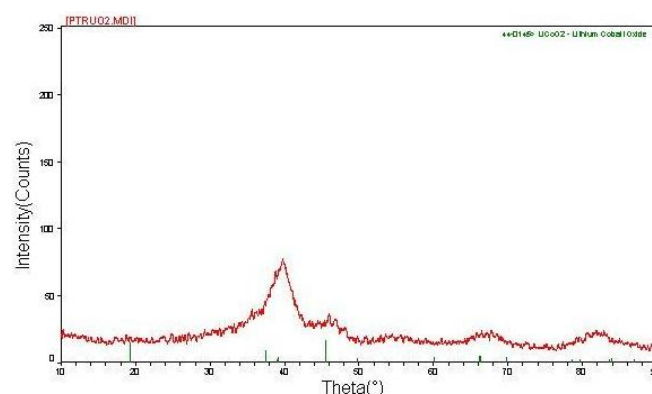


Fig. 6. XRD spectra of Pt deposited on $\text{RuO}_2 \cdot x\text{H}_2\text{O}$ using thermal decomposition method by the means of microwave heating method.

IV. CONCLUSION

Highly dispersed Pt and Pt-Ru deposited on $\text{RuO}_2 \cdot x\text{H}_2\text{O}$ using thermal decomposition by the means of using microwave heating were obtained. Measurement of specific capacitances before and after Pt and Pt-Ru deposition shows that high capacitive property of $\text{RuO}_2 \cdot x\text{H}_2\text{O}$ can be retained in the process by controlling the boiling point of ethylene glycol with the help of adding suitable proportion of de-ionized water. Annealing the temperature to achieve the highest capacitance for $\text{RuO}_2 \cdot x\text{H}_2\text{O}$ should first be obtained for the particular batch of $\text{RuO}_2 \cdot x\text{H}_2\text{O}$ [2]; suitable proportion of ethylene glycol and de-ionized water should then be used to keep the boiling point below the annealing temperature. Cyclic voltammetry, TEM and XRD results confirm the presence of highly dispersed Pt particles on unsupported hydrous ruthenium dioxide. TEM and XRD results also show the absence of any anhydrous $\text{RuO}_2 \cdot x\text{H}_2\text{O}$ in the prepared samples, which proves that $\text{RuO}_2 \cdot x\text{H}_2\text{O}$ remains in hydrous oxide form. Methanol oxidation results show that Pt-Ru alloy deposited on unsupported $\text{RuO}_2 \cdot x\text{H}_2\text{O}$ gives better methanol oxidation activity compared to Pt only deposited on unsupported $\text{RuO}_2 \cdot x\text{H}_2\text{O}$. Future work involves testing the performance of this potential catalytic material i.e. Pt-Ru alloy deposited on unsupported $\text{RuO}_2 \cdot x\text{H}_2\text{O}$, in Direct Methanol fuel cell and check if it improves the dynamic performance of the cell.

ACKNOWLEDGMENT

This work was supported by FSU GAP Program and U.S. Army CERDEC.

REFERENCES

- [1] G. Apanel and E. Johnson, "Direct methanol fuel cells-ready to go commercial?" *Fuel Cells Bulletin*, pp. 12-17, November 2004.
- [2] S. Wasmus and A. Kuver, "Methanol oxidation and direct methanol fuels cells: A selective review," *J. Electroanalytical Chemistry*, vol. 461, pp. 14-31, 1999.
- [3] A. Heinzl and V. M. Barragan, "A review of the state-of-the-art of the methanol crossover in direct methanol fuel cells," *J. Power Sources*, vol. 84, pp. 70-74, 1999.
- [4] P. Agnolucci, "Economics and market prospects of portable fuel cells," *International Journal of Hydrogen Energy*, vol. 32, pp. 4319-4328, 2007.
- [5] C. Y. Chen, J. Y. Shiu, and Y. S. Lee, "Development of a small DMFC bipolar palte stack for portable applications," *Journal of Power Sources*, vol. 159, pp. 1042-1047, 2006.
- [6] J. H. Wee, "Which type of fuel cell is more competitive for portable application: direct methanol fuel cells or direct borohydride fuel cells?" *Journal of Power Sources*, vol. 161, pp. 1-10, 2006.
- [7] U. Krewer and K. Sundmacher, "Transfer function analysis of the dynamic behavior of DMFCs: response to step changes in cell current," *J. Power Sources*, vol. 154, pp. 153-170, 2005.
- [8] P. Argyropoulos, K. Scott, and W. M. Taama, "The effect of operating conditions on the dynamic response of the direct methanol fuel cell," *Electrochimica Acta*, vol. 45, pp. 1983-1998, 2000.
- [9] J. Kallo, J. Kamara, W. Lernert, and R. von Helmut, "Cell voltage transients of a gas-fed direct methanol fuel cell," *J. Power Sources*, vol. 127, pp. 181-186, 2004.

- [10] Q. Ye, T. S. Zhao, and J. G. Liu, "Effect of transient hydrogen evolution/oxidation reactions on the OCV of direct methanol fuel cells," *Electrochem. Solid-State Lett.*, vol. 8, pp. A549-A553, 2005.
- [11] J. H. Yoo, H. G. Choi, J. D. Nam, Y. Lee, C. H. Chung, E. S. Lee, J. K. Lee, and S. M. Cho, "Dynamic behavior of 5-W direct methanol fuel cell stack," *J. Power Sources*, vol. 158, pp. 13-17, 2006.
- [12] A. Payman, S. Pierfederici, and F. Meibody-Tabar, "Energy control of supercapacitor/fuel cell hybrid power source," *Energy Conversion and Management*, vol. 49, pp. 1637-1644, 2008.
- [13] C. Sapienza, L. Andaloro, F. V. Matera, G. Dispenza, P. Creti, M. Ferraro, and V. Antonucci, "Batteries analysis for EC-hybrid powertrain optimization," *International Journal of Hydrogen Energy*, vol. 33, pp. 3230-3234, 2008.
- [14] H. Liu, C. Song, L. Zhang, J. Zhang, H. Wang, and D. Wilkinson, "A review of anode catalysis in the direct methanol fuel cell," *J. Power Sources*, vol. 155, pp. 95-110, 2006.
- [15] K. Lasch, G. Hayn, L. Jorissen, J. Garche, and O. Besenhardt, "Mixed conducting catalyst support materials for direct methanol fuel cell," *J. Power Sources*, vol. 105, pp. 305-310, 2002.
- [16] M. Mastragostino, A. Missiroli, and F. Soavi, "Carbon supports for electrodeposited Pt-Ru catalysts for DMFCs," *J. Electrochem. Soc.*, vol. 151, pp. A1919-A1924, 2004.
- [17] Y. Wang and J. P. Zheng, "A novel monolithic hybrid direct methanol fuel cell," *Electrochem. and Solid-State Lett.*, vol. 10, pp. B26-B30, 2007.
- [18] W. X. Chen, J. Y. Lee, and Z. Liu, "Preparation of Pt and Pt-Ru nanoparticles supported on carbon nanotubes by microwave-assisted heating polyol process," *Materials Lett.*, vol. 58, pp. 3166-3169, 2004.
- [19] J. W. Long, K. E. Swider, C. I. Merzbacher, and D. R. Rolison, "Voltammetric characterization of ruthenium oxide-based aerogels and other RuO_2 solids: The nature of capacitance in nanostructured materials," *Langmuir*, vol. 19, pp. 2532-2532, 2003.
- [20] Y. U. Jeong and A. Manthiram, "Amorphous ruthenium-chromium oxides for electrochemical capacitors," *Electrochem. Solid-State Lett.*, vol. 3, pp. 205-208, 2000.
- [21] I. H. Kim and K. B. Kim, "Ruthenium oxide thin film electrodes for super capacitors," *Electrochem. Solid-State Lett.*, vol. 4, pp. A62-A64, 2001.
- [22] W. Yu, W. Tu, and H. Liu, "Synthesis of nanoscale platinum colloids by microwave dielectric heating," *Langmuir*, vol. 15, pp. 6-9, 1999.
- [23] L. K. Kurihara, G. M. Chow, P. E. Schoen, "Nanocrystalline metallic powders and films produced by the polyol method," *NanoStru. Mater.*, vol. 5, issue 6, pp. 607-613, 1995.



Jim P. Zheng was born in Shanghai, China in 1960. He holds the M.S. and Ph.D. degrees in electrical engineering from the State University of New York at Buffalo in USA, in 1990 and the B.S. in physics from Fudan University in China. He is now a sprint eminent scholar chair professor at the Department of Electrical and Computer Engineering, Florida State University, Florida, USA. He has worked at US Army Research Laboratory at Fort Monmouth, NJ. He has published more than one hundred articles in scholarly journals, and one hundred papers in conference proceedings in the fields of energy storage, fuel cells, nano-sensors, photonics, and thin film growth. He is a senior member of IEEE, and member of JECS, and MRS.



Vivek Tiwari is a senior developer at SAP. He received his B.S. degree in electronics and telecommunication engineering from the College of Engineering Roorkee, India and M.S. degree in electrical engineering from Florida State University, USA. He worked at SmartLinx Solutions and LiDAC. His master thesis is "Formation of $\text{RuO}_2 \cdot x\text{H}_2\text{O}$ -supported Pt anode electrode for direct methanol fuel cells". He has an extensive background

creating cloud-based applications for productivity suites.